ELSEVIER

Catalysis Today 81 (2003) 681–692

CATALYSIS TODAY

www.elsevier.com/locate/cattod

An investigation of alumina-supported catalysts for the selective catalytic oxidation of ammonia in biomass gasification

L.I. Darvell [a], K. Heiskanen [b], J.M. Jones [a,*], A.B. Ross [a], P. Simell [b], A. Williams [a]

[a] *Department of Fuel and Energy, SPEME, University of Leeds, Leeds LS2 9JT, UK*
[b] *VTT Processes, P.O. Box 1601, FIN-02044 VTT, Finland*

Abstract

Alumina-supported catalysts containing different transition metals (Ni, Cu, Cr, Mn, Fe and Co) were prepared and tested for their activity in the selective oxidation of ammonia reaction at high temperatures (between 700 and 900 °C) using a synthetic gasification gas mixture. The catalysts were also characterised for their acidic properties by infrared studies of pyridine and ammonia adsorption and reaction/desorption. The Ni/Al_2O_3 and Cr/Al_2O_3 catalyst displayed the highest selective catalytic oxidation (SCO) activity in that temperature range with excellent N_2 selectivities. FT-IR studies of adsorbed pyridine and NH_3 indicate that Lewis acid sites dominate and that NH_3 adsorption on these sites is likely to be the first step in the SCO reaction. FT-IR studies on less active catalysts, particularly on Cu/Al_2O_3 allowed the detection of oxidation intermediates, amide (NH_2), and possibly hydrazine and imido and nitroxyl species. The amide and hydrazine intermediate gives credence to a proposed SCO mechanism involving a hydrazine intermediate, while the proposed imide, =N–H, and/or nitroxyl, HNO species could be intermediates in incomplete oxidation of NH_3 to N_2O.

Keywords: Selective catalytic oxidation; Mechanism; Ammonia; Alumina; FT-IR spectroscopy; Pyridine

1. Introduction

There is a great deal of interest in the use of biomass as fuel for power production. The most advanced technologies in this field are based on gasification, like the integrated gasification combined cycle (IGCC) technology, which has the potential to generate electricity at a higher efficiency and with lower capital costs than conventional energy conversion technologies. However, despite its advantages, at present, gasification technology is not widely used mainly due to technical problems regarding the removal of undesirable compounds in the gasification gas such as tars, hydrogen sulphide and especially ammonia (NH_3). During gasification of solid fuels, the nitrogen in the fuel is released as different nitrogen compounds (HCN, NO_x, NH_3, etc.), the concentration of these compounds in the product gas depends on the nitrogen content of the feedstock and the gasification process. However it has been found that almost regardless of the gasification process and feedstock used, the predominant compound formed is NH_3, while the share of the other nitrogen compounds is small [1]. The ammonia content of the product gas in different tests has usually been within the range of 100–10,000 ppm [2], hence during combustion of the syngas equivalent amounts of NO_x may be formed. Selective catalytic oxidation (SCO) of ammonia could be used prior to the gas turbine to reduce or perhaps eliminate the amount of NH_3 via the oxidation reaction [3]:

* Corresponding author. Tel.: +44-113-343-2477; fax: +44-113-246-7310.
E-mail address: j.m.jones@leeds.ac.uk (J.M. Jones).

0920-5861/03/$ – see front matter © 2003 Elsevier B.V. All rights reserved.
doi:10.1016/S0920-5861(03)00166-4

$$2NH_3 + \tfrac{3}{2}O_2 \rightarrow N_2 + 3H_2O$$

Several catalysts have been investigated for their activity in the SCO reaction, however, most of these studies have been carried out at low temperatures (<500 °C) [4–8]. Higher temperatures would enable higher process efficiencies. Leppälahti et al. [2,9] studied the activity of different materials in a temperature range of 350–800 °C, finding that alumina gave the best performance with 95% NH_3 conversion achieved at 400 °C. A further study indicated that by adding a small amount of O_2, NH_3 could be oxidised over a higher temperature range (500–700 °C) using alumina as catalyst [10]. Amblard et al. [6,11,12] have studied NH_3 oxidation on heteropolyacids, zeolites, and γ-alumina-supported metals and good selectivities have been achieved at temperatures <650 °C.

The mechanism of NH_3 oxidation and N_2 formation in these processes is still uncertain. Two major routes have been proposed in the literature for the selective oxidation of NH_3 to produce N_2. The first mechanism is the SCO by a direct route involving a hydrazinium-type intermediate [13–15]. The other mechanism is the in situ or "internal" catalytic reduction (iSCR), which involves the oxidation of a significant amount of NH_3 into NO_x, these species can then be reduced by NH_3 molecules to produce N_2 [4,7,11,12,16].

In this paper, we present the results obtained for a range of γ-alumina-supported catalysts, which have been studied for their activity in the SCO reaction and have also been characterised for their acidic properties. Infrared studies of pyridine and ammonia adsorption and reaction/desorption have been conducted in order to gain insight into the sites present on the catalysts and into the ammonia oxidation mechanism.

2. Experimental

2.1. Catalyst preparation

The catalysts were prepared by incipient wetness impregnation of γ-alumina support (BHD, powder form, particle size (70%) 0.063–0.200 mm diameter and a total pore volume of 0.6 $cm^3\,g^{-1}$) with an aqueous solution of a salt of the metal of interest. All the salts used were nitrates obtained from Aldrich Chemical. After impregnation the catalysts were dried stepwise: first overnight at room temperature, and subsequently in an oven at 100 °C for 24 h. Calcination was carried out under flowing air at 700 °C for 4 h. Due to the lower solubility of the chromium nitrate salt, the impregnation of this metal was performed in two steps, with intermediate drying and calcination, in order to obtain the desired chromium concentration.

2.2. Catalyst testing

Catalyst testing was carried out in a laboratory scale continuous fixed bed reactor (i.d. 9 mm), operating at atmospheric pressure and in a temperature range of 700–900 °C. The reactor temperature was monitored by measuring the axial temperature profile from the catalyst bed temperature. The tests were performed by running first the set point at 900 °C and then at 700 °C. measurement of each point took 30–60 min. The reaction mixture (1 $dm^3\,min^{-1}$) was regulated by independent mass flowmeters to simulate a gasification gas of the following composition: CO, 11 vol.%; CO_2, 13.6 vol.%; CH_4, 5.3 vol.%; H_2, 9.6 vol.%; O_2, 3.0 vol.%; H_2O, 12 vol.%; NH_3, 0.44 vol.%; toluene, 0.32 vol.%; N_2, balance. Toluene was used as a tar model compound.

Typically 200 mg of catalyst sample (particle size ≈0.3 mm) was used and it was diluted with silicon carbide (SiC) in a 1:1 volume ratio to reduce the formation of hotspots. The concentrations of effluents with regards to benzene, toluene, N_2O, NO_2, NO, HCN, and NH_3 were measured by on-line FT-IR analysis. The experimental methods are described in more detail in Simell et al. [17].

2.3. Catalyst characterisation

Surface area measurements for the alumina support and all the catalysts prepared for this study have been accomplished by nitrogen adsorption with the three-point BET method, using a Quantasorb (Quantachrome) instrument. Samples of the catalyst prepared were calcined at 900 °C in air, for 1 h, in order to determine their surface areas for comparison purposes.

The infrared spectra of adsorbed bases were obtained at 4 cm^{-1} resolution with a 1750 Perkin-Elmer

FT-IR spectrometer. Approximately 30 mg of sieved catalyst (<0.15 mm) was pressed into self-supporting wafer and placed into a cell connected to a conventional vacuum system that allowed the introduction and evacuation of the adsorbed gases/vapours. The cell allowed the simultaneous study of six different catalysts. In three separate series of experiments, prior to adsorption of the bases, the wafers were cleaned by heating in O_2 at 500, 600 and 700 °C for 3 h followed by outgassing at the same temperature for 1 h. The spectra of the clean wafers were recorded as backgrounds. Identical features were observed at these three calcination temperatures and only the results for cleaning at 700 °C are presented here. Pyridine (Sigma-Aldrich) was degassed by successive freeze/pump/thaw cycles prior to adsorption. The pyridine (Py) vapour was admitted in the preheated cell (at 100 °C) for ∼1 min and was left to equilibrate for 1 h prior to evacuation for 30 min to remove any physisorbed species. In a separate series of experiments, ammonia (20 mm Hg) (Linde Gas, UK) was contacted with the wafers at room temperature for 30 min and then evacuated for 30 min prior to recording the spectra. Spectra of adsorbed bases were obtained by subtraction of the appropriate background (clean wafer) spectrum from that of the wafer + base spectrum. Spectra were recorded after desorbing the wafers for 30 min at successively higher temperatures until either a flat spectrum was observed (i.e. complete desorption) or until the sample became opaque to the infrared.

X-ray powder diffraction patterns, of the Cu/Al_2O_3 catalysts (calcined at 700 and 900 °C), were obtained with an APD 1700 powder diffractometer employing Cu Kα radiation ($\lambda = 1.5406$ Å). The X-ray was operated at 40 kV and 30 mA. Diffraction patterns were obtained using a scanning rate of 0.01 °/s and were recorded over $5^\circ < 2\theta < 95^\circ$ angles.

3. Results

3.1. Catalyst characterisation

Table 1 lists the catalysts prepared for this study including the results of the surface area determinations at both calcination temperatures, 700 and 900 °C (percentages refer to the weight percent of metal present).

Fig. 1 shows the XRD spectra of Cu/Al_2O_3 calcined at 700 and 900 °C. The sample calcined at 700 °C show the diffraction lines typical for the CuO phase as indicated by the two peaks at $2\theta \sim 35.4^\circ$ and 38.6° [18]. It is known that at high Cu loading and low calcination temperature, bulk-like CuO forms. A higher calcination temperature like 900 °C leads to the formation of $CuAl_2O_4$ [18]. As shown in Fig. 1 no CuO peak is detected for the catalyst calcined at 900 °C. However, there is difficulty in determining incipient copper aluminate formation because both the aluminate and the γ-alumina are spinel-type phases and their X-ray patterns are very similar.

3.2. Catalytic activity

Table 2 shows the conversion of ammonia and toluene achieved with the catalysts at 700 and 900 °C. All catalysts displayed excellent selectivity to N_2 under the conditions studied and only trace amounts of oxidised N-compounds were observed. Ni/Al_2O_3 shows an excellent performance with 99% conversion of nitrogen compounds at 900 °C. At 700 °C, the temperature of interest, Cr/Al_2O_3 gives the best

Table 1
Catalysts prepared and their surface area

Catalyst	Metal loading (wt.%)	Surface area at 700 °C (m^2/g)	Surface area at 900 °C (m^2/g)	Impregnating salt
Al_2O_3	–	155	87	–
NiO/Al_2O_3	10	111	77	$Ni(NO_3)_2{\cdot}6H_2O$
CuO/Al_2O_3	10	95	47	$Cu(NO_3)_2{\cdot}\frac{5}{2}H_2O$
Cr_2O_3/Al_2O_3	10	85	53	$Cr(NO_3)_3{\cdot}9H_2O$
Mn_2O_3/Al_2O_3	7	100	55	$Mn(NO_3)_2{\cdot}4H_2O$
Fe_2O_3/Al_2O_3	8.5	104	42	$Fe(NO_3)_3{\cdot}9H_2O$
Co_3O_4/Al_2O_3	10	87	59	$Co(NO_3)_2{\cdot}6H_2O$

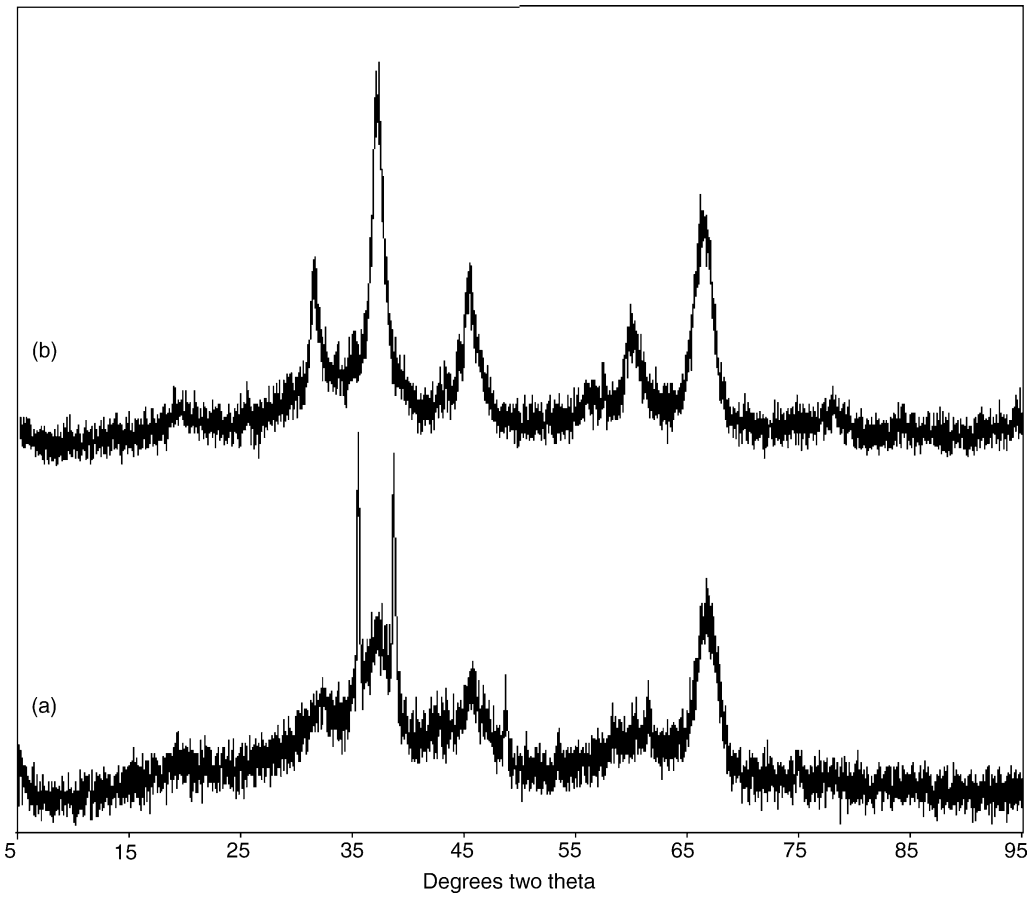

Fig. 1. XRD patterns measured for Cu/Al_2O_3 calcined at: (a) 700 °C; (b) 900 °C.

conversion at 70%. In general the performances of most of the metal catalysts seem to be enhanced by the temperature increase, except for the Cr/Al_2O_3 and Cu/Al_2O_3 catalysts. A possible explanation of decreasing ammonia conversion with increasing temperature is that the surface oxygen sites needed for ammonia oxidation are consumed by the competing H_2 and CO oxidation reactions. Certainly copper is well known as a good H_2 oxidation catalyst [19]. Previous studies suggest that all catalysts have a temperature window for ammonia conversion [20]. Another possibility is that these two catalysts form catalytically inactive phases at higher temperature. Surface areas are seen to decrease after calcinations at 900 °C for all the catalysts (Table 1). Also, the XRD data presented in Fig. 1 for the Cu/Al_2O_3 catalysts does indicate structural changes but is inconclusive concerning $CuAl_2O_4$ formation. Furthermore, this structural change does not appear to adversely affect the catalyst activity—upon reducing the temperature in the NH_3 oxidation experiments from

Table 2
Ammonia and toluene conversion at 700 and 900 °C

Catalyst	NH_3 conversion (%)		Toluene conversion (%)	
	700 °C	900 °C	700 °C	900 °C
Al_2O_3	34	16	9	48
10% Ni/Al_2O_3	44	99	100	99
10% Cu/Al_2O_3	40	27	22	76
10% Cr/Al_2O_3	70	58	17	22
7% Mn/Al_2O_3	17	32	30	82
8.5% Fe/Al_2O_3	3	19	23	65
10% Co/Al_2O_3	19	77	19	96

900 to 700 °C, the ammonia conversion increases back to approximately 40%. Therefore, competing reactions that consume available surface oxygen is a more plausible explanation. Future work by this group concerning kinetic model development will give more insight into the behaviour of these competing reactions. Regarding toluene, the Ni/Al_2O_3 catalyst also shows the best toluene conversion at both temperatures. In the case of toluene oxidation all the catalysts have improved activities at the higher temperature.

3.3. Adsorption of pyridine

Pyridine adsorption spectra were recorded for the Ni/Al_2O_3, Co/Al_2O_3, Cu/Al_2O_3, Mn/Al_2O_3 catalysts, as well as the alumina support for comparison. Furthermore, the influence of desorption temperature was also investigated. Catalysts containing Ni and Co showed essentially the same behaviour and typical spectra for the Co/Al_2O_3 catalyst are shown in Fig. 2(a). The results for the alumina support, are shown in Fig. 2(b) for comparison purposes. In Fig. 2(a) and (b), the characteristic band for pyridine adsorbed on Lewis acid sites can be observed at $\sim$1450 cm^{-1}, and there is no evidence of pyridine adsorbed on Brønsted acid sites, which would be indicated by a band at 1540 cm^{-1} [21]. Increasing desorption temperature results in a decrease in band intensities with no transformation of the pyridine.

The behaviour of the pyridine during desorption from the Mn/Al_2O_3 and Cu/Al_2O_3 showed quite different behaviour. The spectra showing the interactions of pyridine on the surface of Mn/Al_2O_3 after desorption at different temperatures can be seen in Fig. 3(a). The characteristic bands for pyridine adsorbed on Lewis acid sites can also be seen in the spectra of this catalyst for desorption temperatures below 200 °C. As for the other catalysts there is no indication of Brønsted acidity. However at desorption above 200 °C, the spectra become more complex. A broad band appears at $\sim$1560–1555 cm^{-1}, and its intensity increases with the desorption temperature up to 500 °C. After evacuation at 300 °C a shoulder at $\sim$1505 cm^{-1} and a new band at $\sim$1635 cm^{-1} appear, which persists up to $\sim$500 and >600 °C, respectively. Also at 500 °C the band at 1450 cm^{-1} changes its shape, becoming much broader, shifting to a higher wavenumber and having an apparent increased intensity.

The spectra of pyridine adsorbed on Cu/Al_2O_3 at different desorption temperatures are shown in Fig. 3(b). Only the spectra corresponding to three desorption temperatures are presented in this figure, as the sample wafer became opaque to the IR after evacuation at 400 °C hence no spectra could be recorded thereafter. The characteristic band of pyridine adsorbed on Lewis acid sites observed in the previous catalysts is also shown after degassing at 100 °C, and there is no indication of pyridine on Brønsted acid sites. However, after desorption at 200 °C, the spectra become more complex and the bands are very intense. The band at $\sim$1610 cm^{-1} is shifted to a higher frequency and its intensity increases significantly with the desorption temperature. The new bands found in the spectra of pyridine adsorbed on Mn/Al_2O_3 can also be observed for the Cu/Al_2O_3 catalyst, although with higher intensity. The intensities of these bands at 1505–1490 cm^{-1}, 1560–1555 cm^{-1} and also of the band resulting from adsorption of pyridine on Lewis acid sites (at 1450 cm^{-1}) are significantly increased after outgassing at 200 and 300 °C.

3.4. Adsorption of ammonia

The IR spectra showing the interactions of ammonia on the surface of the alumina support calcined at 700 °C are shown in Fig. 4(a). The two main bands observed near 1620 and 1240 cm^{-1} result from coordinated ammonia on Lewis acid sites. The IR spectra of ammonia adsorbed on the surface of Co/Al_2O_3, Mn/Al_2O_3, Fe/Al_2O_3, and Cr/Al_2O_3 catalysts calcined at 700 °C were very similar to those of the Mn/Al_2O_3 spectra shown in Fig. 4(b). These spectra present the same bands found on those of the ammonia adsorbed on alumina and indicate that ammonia is sequentially desorbed from stronger Lewis acid sites as the temperature is increased. It can also be observed that in Fig. 4(b) that the bands resulting from ammonia adsorption on Lewis acid sites decrease in intensity after evacuation at 200 °C.

The IR spectra of ammonia adsorbed on Cu/alumina calcined at 700 °C showed unique desorption behaviour as presented in Fig. 5. The Lewis acid

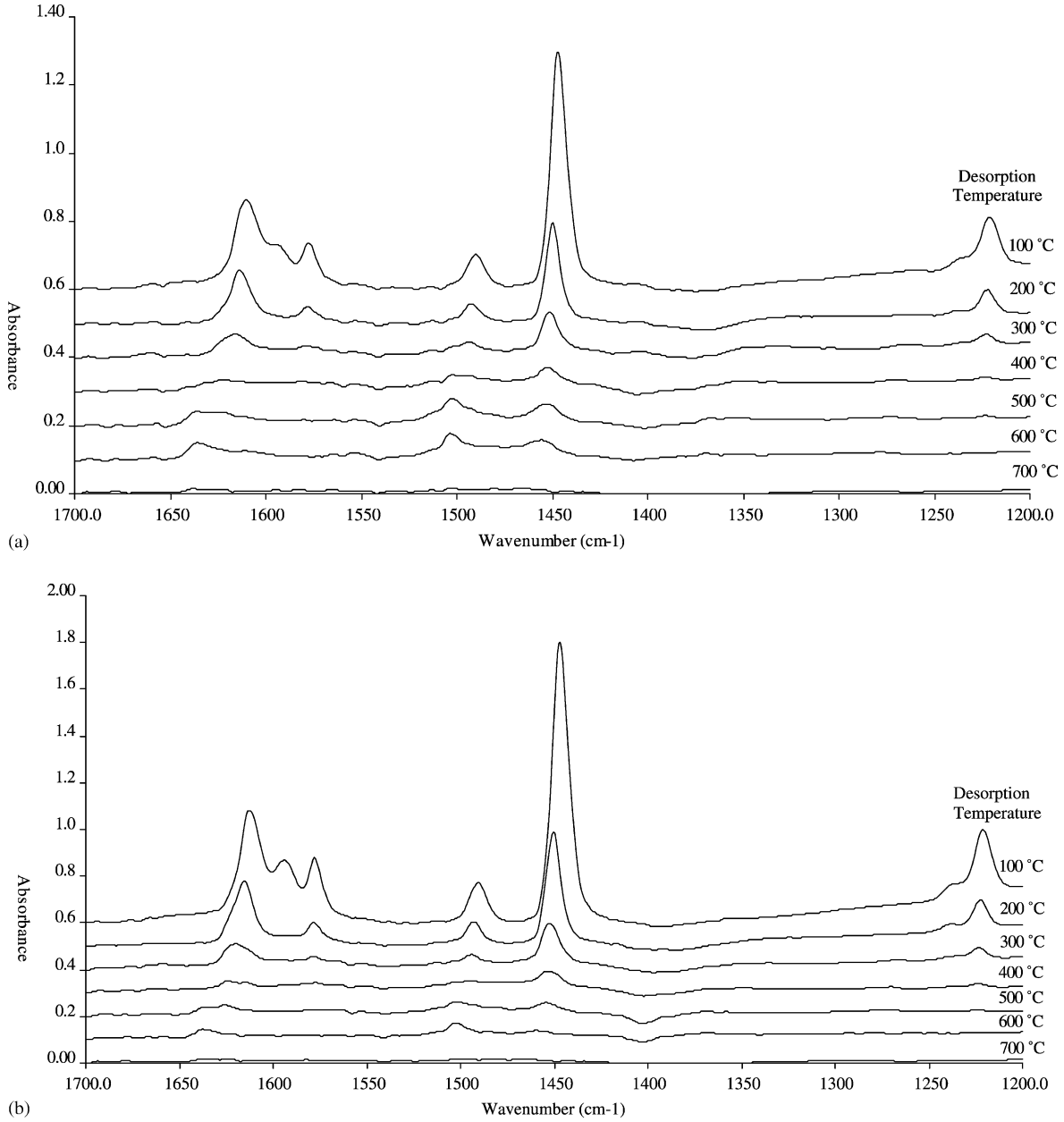

Fig. 2. (a) Spectra of pyridine adsorbed on Co/alumina calcined at 700 °C, desorbed at various temperatures; (b) spectra of pyridine adsorbed on alumina calcined at 700 °C, desorbed at various temperatures. Spectra has been offset for clarity.

sites resulting in the bands at 1620 and 1240 cm^{-1} discussed previously decrease in intensity after evacuation at 200 °C, while a new strong band appears at ~1490 cm^{-1} together with a very weak band at ~1553 cm^{-1}. When these bands appear the intensity of the band at 1450 cm^{-1} increases significantly, all these bands disappear after outgassing at a higher temperature.

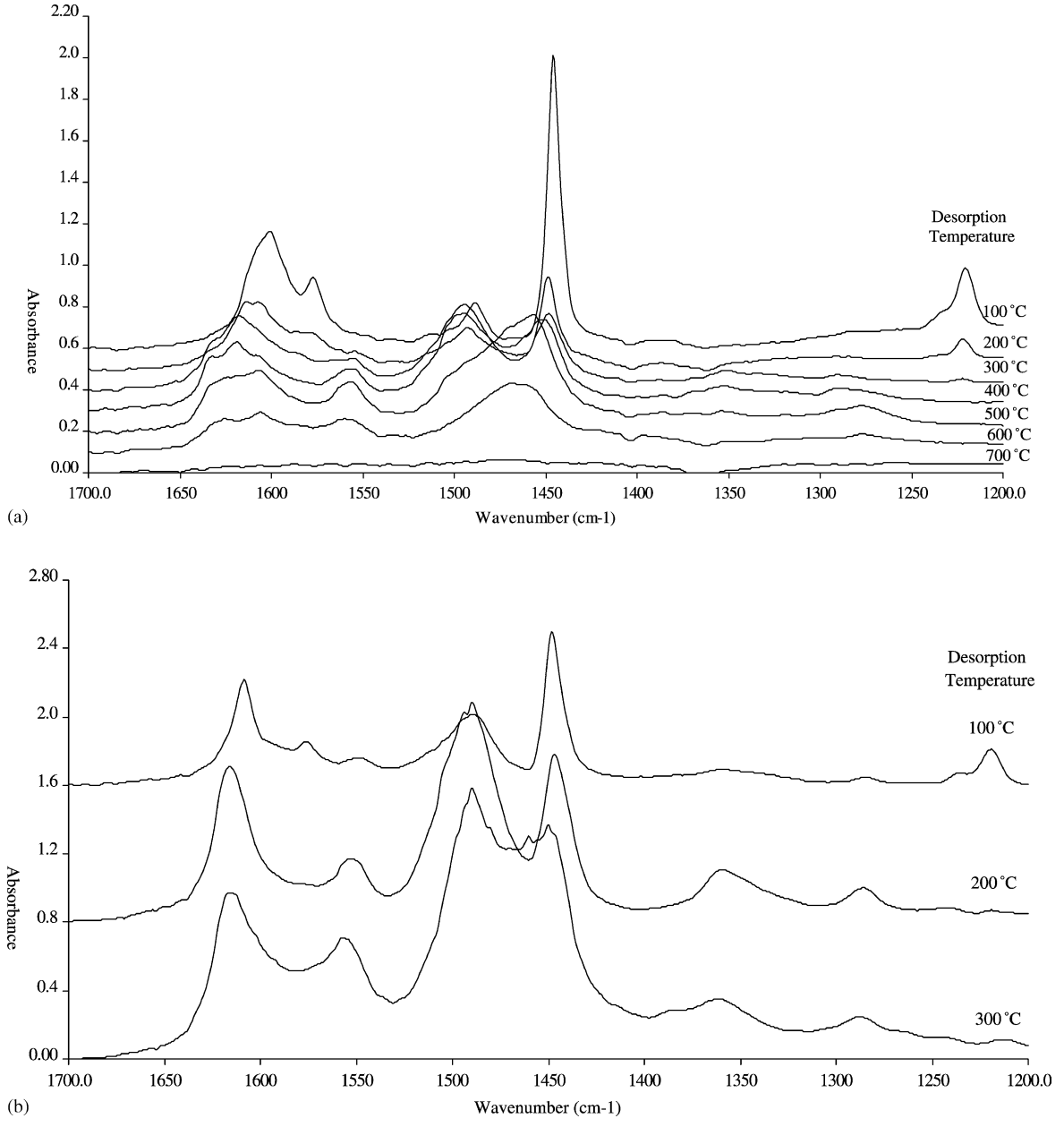

Fig. 3. (a) Spectra of pyridine adsorbed on Mn/alumina calcined at 700 °C, desorbed at various temperatures; (b) spectra of pyridine adsorbed on Cu/alumina calcined at 700 °C, desorbed at various temperatures. Spectra has been offset for clarity.

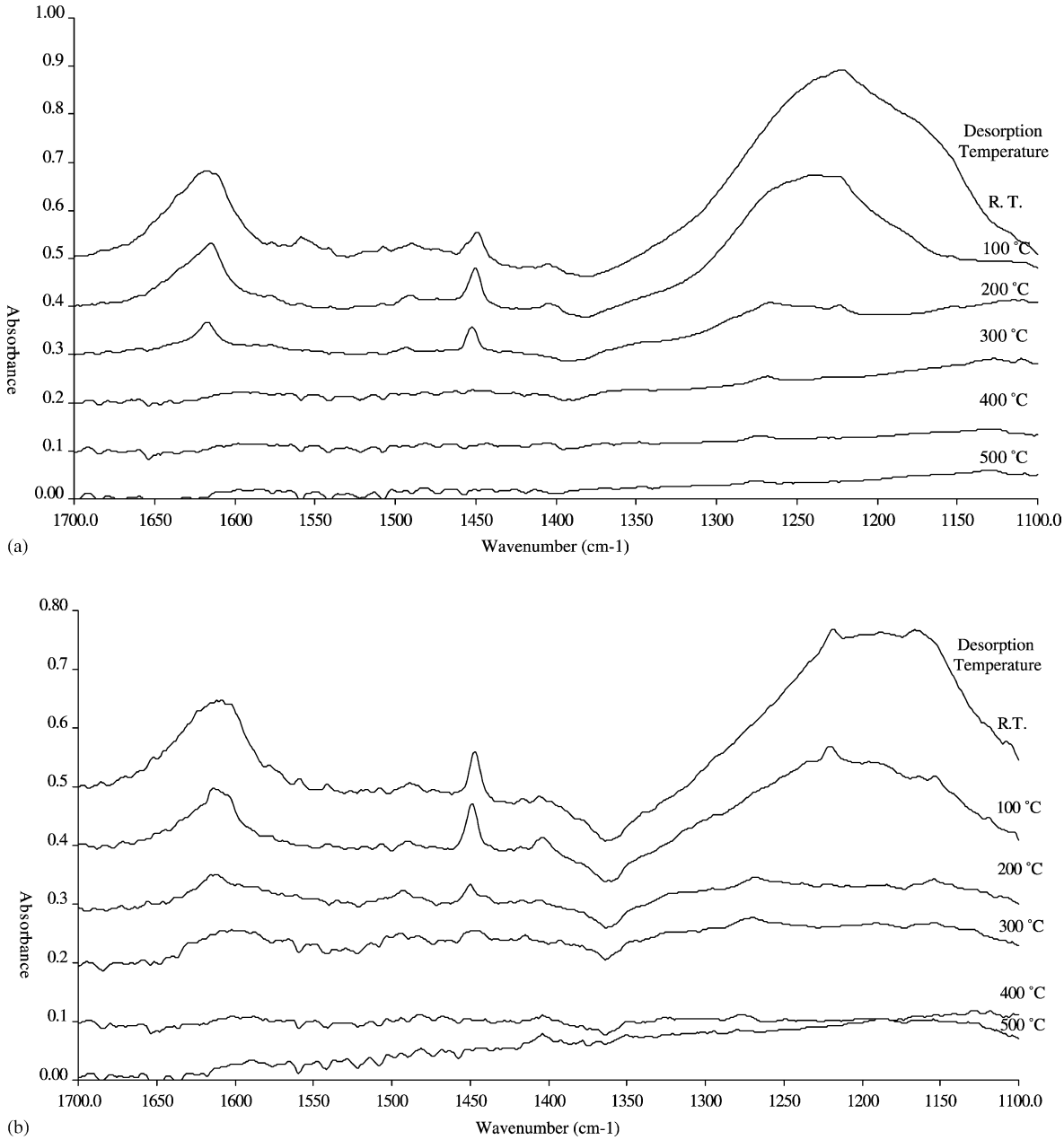

Fig. 4. (a) Spectra of ammonia adsorbed on alumina calcined at 700 °C, desorbed at various temperatures; (b) spectra of ammonia adsorbed on Mn/alumina calcined at 700 °C, desorbed at various temperatures. Spectra has been offset for clarity (R.T.: room temperature).

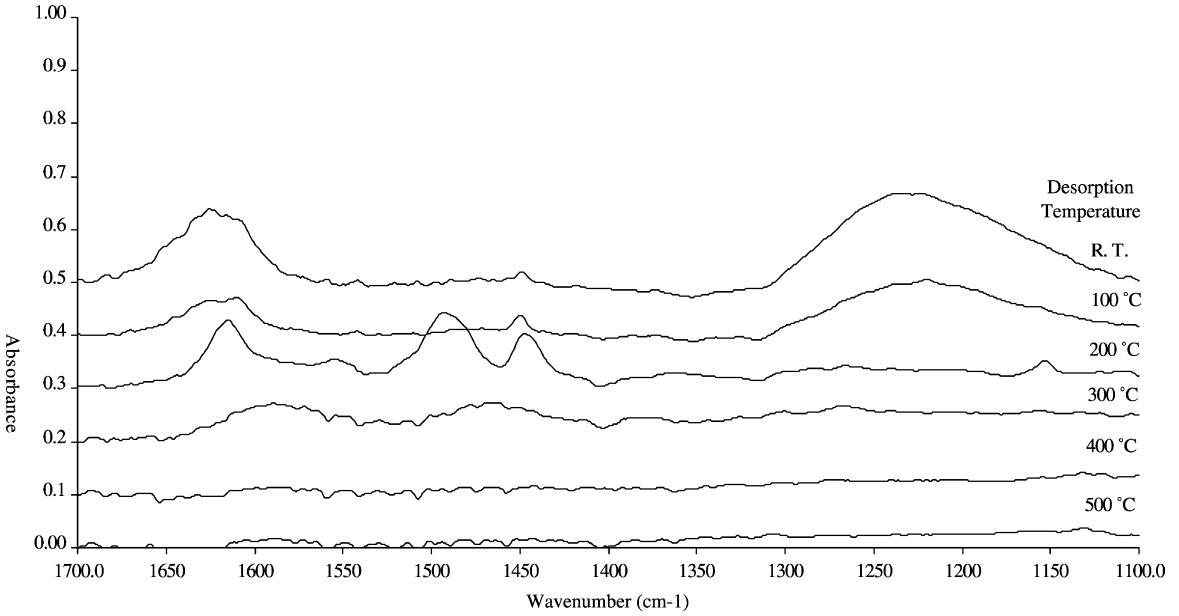

Fig. 5. Spectra of ammonia adsorbed on Cu/alumina calcined at 700 °C, desorbed at various temperatures. Spectra has been offset for clarity (R.T.: room temperature).

4. Discussion

4.1. Adsorption of pyridine

All the catalysts displayed spectra typical of pyridine adsorbed on Lewis acid sites, and for all but the Mn/Al_2O_3 and Cu/Al_2O_3 catalysts, this pyridine was desorbed unchanged when the temperature was increased. In the case of the Mn/Al_2O_3 and Cu/Al_2O_3 catalysts the spectra become more complex upon increasing the desorption temperature (Fig. 3(a) and (b)) indicating transformation of the adsorbed pyridine. This transformation results in shifting of the ring vibration bands to higher wavenumber, together with an increase in intensity particularly for the case of the Cu/Al_2O_3 catalysts. A shift to higher frequency of ring vibration is indicative of increasing coordinative bond strength. It is likely from the broadness of the bands that a mixture of adsorbed species are present on the Mn/Al_2O_3 and Cu/Al_2O_3 catalysts after desorption at 200 °C, i.e. some of the pyridine associated with Lewis acid sites changes its bonding environment. A number of other species have been postulated for pyridine adsorption on acid surfaces. The pyridinium ion gives rise to ring vibrations at 1500–1485, ~1620 and 1640 cm^{-1} and the N^+–H bend appears at 1540 cm^{-1} [21]. While the spectra displayed in Fig. 3(a) and (b), after degassing at >200 °C are reminiscent of pyridine on Brønsted acid sites they are not typical.

A new band at 1635 cm^{-1} is apparent in Fig. 3(a) after desorption at 300 °C. Knözinger [22] studied pyridine adsorption on δ- and η-Al_2O_3 and postulated an additional surface reaction between pyridine and surface OH groups takes place at temperatures higher than roughly 350 °C to explain the appearance of a new band at 1635 cm^{-1}. This interaction was considered to lead to a surface pyridine species with a C=O stretching band at 1634 cm^{-1} and the reaction has been described by

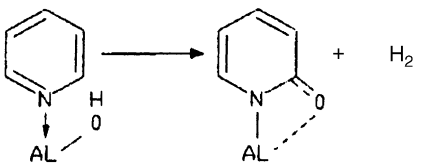

The ring vibrations of pyridine could also be contributing to the spectra at temperatures >200 °C

in Fig. 3(a) and (b), since they give rise to bands in the same regions (1645–1590, 1540–1470, and 1440–1410 cm^{-1}) [23].

A second oxidation product, pyridine-N-oxide has been proposed based on the photoacustic FT-IR spectroscopy of pyridine on γ-Al_2O_3 [24]. These species give rise to bands at 1464, 1498 and 1608 cm^{-1}, while the N–O stretch appears at ∼1260 cm^{-1}. A clear band is observed in this region (1280–1270 cm^{-1}) for both Mn/Al_2O_3 and Cu/Al_2O_3 catalysts, which is absent in the analogous spectra for pyridine adsorbed on alumina.

While at this stage it is not possible to give unequivocal assignment to the bands in Fig. 3(a) and (b) there is some evidence that oxidation of pyridine is occurring. Thus copper and manganese facilitate oxygen transfer to the adsorbed pyridine.

4.2. Adsorption of ammonia

Although we recognise that the experimental conditions for the IR work are not the same as those used during the catalytic testing (i.e. no oxygen was added simultaneously with the ammonia, etc.), evidence of oxidation reactions were found as some ammonia surface transformations were observed. These surface transformations could give an idea of the type of reactions that take place (between the ammonia and oxygen) over the catalyst surface at the operating temperature. It is likely that the oxygen treatment prior to the ammonia adsorption resulted in oxidised surface species being available to react with the ammonia. However the effect of the other gases present in the mixture is not considered at this point. It is clear from Fig. 5 that adsorbed ammonia on Cu/Al_2O_3 has been transformed after a temperature of 200 °C. New bands at ∼1490, and at ∼1553 cm^{-1} appear while the band at ∼1450 cm^{-1} becomes more intense. Similar bands have been observed in previous studies of ammonia adsorption on CuO/TiO_2 [15,25], ammonia and hydrazine adsorption on Fe_2O_3/TiO_2 [26,27], and ammonia and hydrazine adsorption over anatase supported metal oxides [14]. A very weak band at 1555 cm^{-1} has been detected, after outgassing at 423 K, during ammonia adsorption experiments over Fe_2O_3/TiO_2, this band was assigned to the NH_2 amide species [26,27].

Regarding the new strong band that appears at ∼1490 cm^{-1}, and the increase in intensity of the band at 1450 cm^{-1} after outgassing at 200 °C, similar bands have been reported in previous studies of ammonia adsorption on CuO/TiO_2 [15,25], and of ammonia and hydrazine adsorption on Fe_2O_3/TiO_2 [26,27] and on anatase supported metal oxides [14], but have not been reported before, on alumina-supported catalysts. The spectra recorded, in the latter studies, after evacuation of adsorbed hydrazine at 423 °C and increasing temperatures are very similar to those observed after ammonia adsorption and transformation over the Fe_2O_3/TiO_2 surface by heating at the same temperature and also to those observed in Fig. 5 at 100 °C and increasing temperatures. It was suggested that adsorbed hydrazine could be formed from adsorbed ammonia on the surface of the catalysts which then reacts to form the products that result in the bands observed at ∼1480 and 1450 cm^{-1}. It was also observed that these bands seem to belong to two different species because they behave independently of each other, i.e. one of these species is formed first and disappears later and is characterised by a band at 1450 cm^{-1}; the other is formed later and is characterised by a band at 1480 cm^{-1}. Since this band formed at slightly higher temperature and disappeared easily, a reactive intermediate was inferred. The behaviour described above is almost identical to the behaviour reported here for the Cu/Al_2O_3 catalyst. Two explanations have been proposed to explain these observations. One is that these bands result from two species, one being an imido =N–H species [15] responsible for the band at 1450 cm^{-1} and another species responsible for the band at 1480 cm^{-1}, which could be an adsorbed nitroxyl HNO species [14,15] as this band has been tentatively assigned to the NO stretching of such species. Alternatively, HNO could be responsible for both bands since it has been proposed that the nitroxyl species when adsorbed can be responsible for a stretching band similar to that of other N=O containing species in the 1550–1400 cm^{-1} range, and for a NH bending like band for secondary amines, in the 1450–1400 cm^{-1} region [14]. Since the bands appear and disappear at different temperatures this explanation is less likely. It is to be observed that the nitroxyl species has been proposed as one of the intermediate species for ammonia oxidation to N_2O by the following mechanism [26]:

$$–NH_2 \rightleftarrows –NH + H^+ + e^-$$

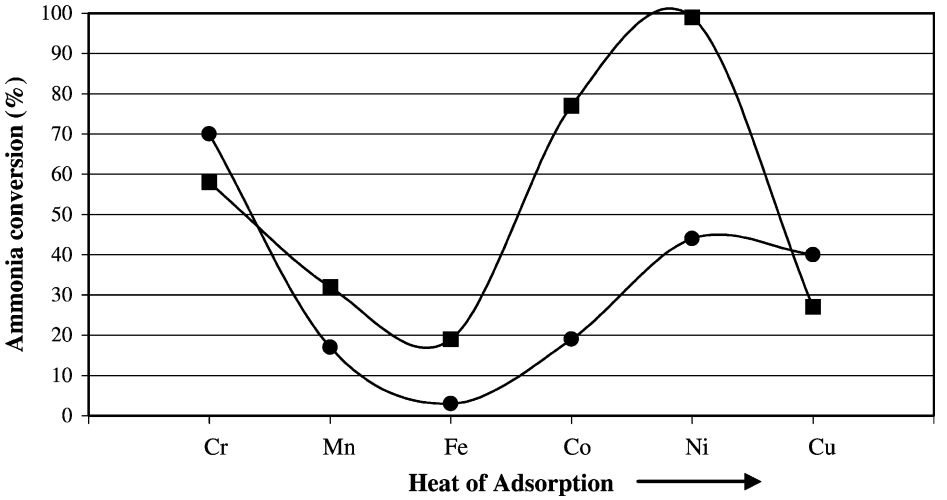

Fig. 6. Volcano plots for ammonia conversion at 700 and 900 °C by alumina-supported transition metals. Transition metals are in order of increasing heat of adsorption (as ordered in the periodic table). (●) Activity at 700 °C; (■) activity at 900 °C.

$$\text{–NH} + \tfrac{1}{2}\text{O}_2 \rightleftarrows \text{HNO} + 2\text{e}^-$$

$$2\text{HNO} \rightleftarrows \text{N}_2\text{O} + \text{H}_2\text{O}$$

The intermediate products detected so far, in particular amide (NH_2) species and hydrazine (N_2H_4) species seem to support one of the mechanisms proposed in the literature for the SCO reaction leading to the production of N_2. Such mechanism is presented below and has been proposed for ammonia molecules reacting over the surfaces of Fe_2O_3/TiO_2, CrO_x/TiO_2, CoO_x/TiO_2 and CuO/TiO_2 [14,15]:

$$\text{NH}_3\,(\text{g}) \rightarrow \text{NH}_3\,(\text{ads}) \quad \text{(adsorption on acid sites)}$$

$$\text{NH}_3\,(\text{ads}) + \text{M}^{n+} \rightarrow \text{NH}_2\,(\text{ads}) + \text{M}^{(n-1)+} + \text{H}^+\ \text{(redox)}$$

$$2\text{NH}_2\,(\text{ads}) \rightarrow \text{N}_2\text{H}_4\,(\text{ads})$$

$$\text{N}_2\text{H}_4\,(\text{ads}) + 4\text{M}^{n+} \rightarrow \text{N}_2 + 4\text{M}^{(n-1)+} + 4\text{H}^+\ \text{(redox)}$$

$$2\text{M}^{(n-1)+} + \tfrac{1}{2}\text{O}_2 + 2\text{H}^+ \rightarrow 2\text{M}^{n+} + \text{H}_2\text{O}$$

The evidence presented here suggests that the hydrazine decomposition mechanism is important under conditions where there is little, or limited oxygen available. In the spectroscopic studies the only oxygen available was that associated with the metal oxide catalysts, and the catalyst testing is carried out in an essentially reducing environment. At higher O_2 concentrations, the iSCR mechanism may become more important, as suggested by other researchers for SCO in a strongly oxidising environment.

It is interesting that ammonia oxidation intermediates were only observed over the Cu/Al_2O_3 catalyst, and possibly pyridine oxidation products observed on the Mn/Al_2O_3 and Cu/Al_2O_3 catalysts. Fig. 6 shows the relationship between activity in the NH_3 oxidation reaction and position in the transition series (transition metals ordered in terms of increasing heat of adsorption). For a catalyst to be active in a reaction, both surface atoms and adsorbates must participate to form a surface chemical bond. The strength/nature of the bond depends on the heat of adsorption, among other variables. As the heat of adsorption generally increases from right to left in the periodic table [28], a relation between the activity and the heat of adsorption is often found. In Fig. 6 a volcano type plot is seen from Mn to Cu. Cu/Al_2O_3 shows moderate activity in the SCO reaction and it could be that in these instances the ammonia oxidation rate is optimum for the detection of intermediates by FT-IR studies.

A very important observation is that neither pyridine nor ammonia adsorption showed any appreciable Brønsted acidity on the surfaces of the active catalysts, nor on that of the alumina. This is in agreement

with previous works in which had been concluded that Brønsted acidity is not directly involved nor required in the SCO reaction [14,15].

5. Conclusions

Of the catalysts studied the Ni/Al_2O_3 and Cr/Al_2O_3 displayed the highest SCO activity in the 700–900 °C range for a synthetic gasification gas mixture. FT-IR studies of adsorbed pyridine and NH_3 indicate that Lewis acid sites dominate and that NH_3 adsorption on these sites is likely to be the first step in the SCO reaction. FT-IR studies on less active catalysts, particularly on Cu/Al_2O_3 allowed the detection of oxidation intermediates, amide (NH_2), and possibly hydrazine and imido and nitroxyl species. The amide and hydrazine intermediates give credence to a proposed SCO mechanism involving a hydrazine intermediate, while the proposed =N–H and/or HNO species could be intermediates in incomplete oxidation of NH_3 to N_2O.

Acknowledgements

This work is part of the EESD programme, funded by the European Community under contract no. ERK5-CT-1999-00020, “Ammonia Removal”.

References

[1] J. Leppälahti, T. Koljonen, Fuel Process. Technol. 43 (1) (1995) 1.
[2] J. Leppälahti, T. Koljonen, M. Hupa, P. Kilpinen, Energy Fuels 11 (1) (1997) 30.
[3] M. Amblard, R. Burch, B.W.L. Southward, Catal. Today 59 (2000) 365.
[4] N.N. Sazonova, A.V. Simakov, T.A. Nikoro, G.B. Barannik, V.F. Lyakhova, V.I. Zheivot, Z.R. Ismagilov, H. Veringa, React. Kinet. Catal. Lett. 57 (1) (1996) 71.
[5] L. Gang, J. van Grondelle, A.B. Anderson, R.A. van Santen, J. Catal. 186 (1999) 100.
[6] M. Amblard, R. Burch, B.W.L. Southward, Appl. Catal. B 22 (3) (1999) L159.
[7] R.Q. Long, R.T. Yang, Chem. Commun. (2000) 1651.
[8] L. Gang, A.B. Anderson, J. van Grondelle, R.A. van Santen, W.J.H. van Gennip, J.W. Niemantsverdriet, P.J. Kooyman, A. Knoester, H.H. Brongersma, J. Catal. 206 (2002) 60.
[9] J. Leppälahti, T. Koljonen, M. Hupa, P. Kilpinen, Energy Fuels 11 (1) (1997) 39.
[10] J. Leppälahti, P. Kilpinen, M. Hupa, Energy Fuels 12 (4) (1998) 758.
[11] M. Amblard, R. Burch, B.W.L. Southward, Catal. Lett. 68 (2000) 105.
[12] R. Burch, B.W.L. Southward, Chem. Commun. (1999) 1475.
[13] M. Trombetta, G. Ramis, G. Busca, B. Montanari, A. Vaccari, Langmuir 13 (1997) 4628.
[14] J.M.G. Amores, V. Sanchez Escribano, G. Ramis, G. Busca, Appl. Catal. B 13 (1997) 45.
[15] G. Ramis, L. Yi, G. Busca, Catal. Today 28 (1996) 373.
[16] R. Burch, B.W.L. Southward, J. Catal. 195 (2000) 217.
[17] P.A. Simell, A.K. Hakala, H.E. Haario, A.O.I. Krause, Ind. Eng. Chem. Res. 36 (1997) 42.
[18] R.M. Friedman, J.J. Freeman, F.W. Lytle, J. Catal. 55 (1978) 10.
[19] J.F. Le Paige, Applied Heterogeneous Catalysis: Design-Manufacture, Use of Solid Catalysts, Editions Technip, Paris, 1987, p. 55.
[20] J. Leppälahti, E. Kurkela, P. Simell, P. Ståhlberg, Formation and removal of nitrogen compounds in gasification processes, in: A.V. Bridgewater (Ed.), Advances in Thermochemical Biomass Conversion, vol. 1, Blackie, Glasgow, 1994, pp. 160–174.
[21] E.P. Parry, J. Catal. 25 (1963) 371.
[22] H. Knözinger, Adv. Catal. 25 (1976) 184.
[23] A.R. Katritzky, Handbook of Heterocyclic Chemistry, Pergamon Press, Oxford, 1985, p. 41.
[24] M.W. Urban, J.L. Koenig, Appl. Spectrosc. 40 (6) (1986) 851.
[25] G. Ramis, L. Yi, G. Busca, M. Turco, E. Kotur, R.J. Willey, J. Catal. 157 (1995) 523.
[26] G. Ramis, M.A. Larrubia, G. Busca, Top. Catal. 11/12 (2000) 161.
[27] M.A. Larrubia, G. Ramis, G. Busca, Appl. Catal. B 30 (2001) 101.
[28] G.A. Somorjai, Introduction to Surface Chemistry and Catalysis, Wiley, New York, 1994, pp. 401–402.